**J. Cent. South Univ.** (2024) 31: 1371−1382
**DOI:** https://doi.org/10.1007/s11771-024-5624-5

Springer

# Heavy metal pollution and ecological risk assessment: A study on Linli County soils based on self-organizing map and positive factorization approaches

ZOU Hao(邹昊)[1], LI Wu-qing(李武清)[2], REN Bo-zhi(任伯帜)[1, 4]*,
XIE Qing(谢青)[3], CAI Zhao-qi(蔡昭奇)[4], CHEN Lu-yuan(陈禄源)[4], WANG Jin(王瑾)[5]

1. School of Civil Engineering, Hunan University of Science and Technology, Xiangtan 411201, China;
2. Institute of Geological Survey of Hunan Province, Changsha 410083, China;
3. School of Resource Security, Hunan University of Science and Technology, Xiangtan 411201, China;
4. School of Earth Science and Spatial Information, Hunan University of Science and Technology, Xiangtan 411201, China;
5. College of Foreign Languages, Hunan University, Changsha 410082, China



**Abstract:** This study analyzed the pollution level, distribution, sources, and ecological impact of six heavy metals (As, Cd, Cr, Cu, Zn and Pb) in soil from Linli County, China. The concentration analysis showed that the concentration of Cd in all samples exceeded the background value, and the exceeding rate reached 100%, while the average concentrations of other elements were similar to the background value, and the exceeding rate was under 15%. The pollution level of Cd was the most severe according to geo-accumulation index and enrichment factor, while other elements were under mild pollution level. The results of self-organizing map (SOM) and positive matrix factorization (PMF) analysis showed that agricultural activities were one of the main sources of heavy metal elements in soil, and natural weathering and industrial pollution could also lead to soil pollution. Cd appeared to be the most significant pollutant element in the soil of Linli County, and it had the largest impact on the ecological environment. Overall, this study provides guidance for soil pollution control and related policies, aiming to reduce the pollution of heavy metal elements in soil and the hazards to the ecological system caused by agricultural production and industrial activities.

**Key words:** ecological risk; positive matrix factorization; heavy metals pollution; soil; self-organizing maps

**Cite this article as:** ZOU Hao, LI Wu-qing, REN Bo-zhi, XIE Qing, CAI Zhao-qi, CHEN Lu-yuan, WANG Jin. Heavy metal pollution and ecological risk assessment: A study on Linli County soils based on self-organizing map and positive factorization approaches [J]. Journal of Central South University, 2024, 31(4): 1371−1382. DOI: https://doi.org/10.1007/s11771-024-5624-5.

## 1 Introduction

In recent decades, rapid economic development has led to increasingly serious contamination of heavy metals (HMs) in soils, resulting in growing concern about the negative impacts of soil contamination [1, 2]. Various studies on the environmental contamination of HMs in typical areas have indicated that the current levels of HMs

ZOU Hao and LI Wu-qing contributed equally to this work.

**Foundation item:** Project(41973078) supported by the National Natural Science Foundation of China; Project(2022SK2073) supported by the Hunan Provincial Natural Science Foundation, China
**Received date:** 2023-12-25; **Accepted date:** 2024-02-01

**Corresponding author:** REN Bo-zhi, PhD, Professor; E-mail: bozhiren@126.com; ORCID: https://orcid.org/0000-0002-9797-7314

in soils are much higher than the previous environmental standard limits, especially for Hg, Cd and Pb [3 − 5]. The cumulative damage of HMs to the soil environment is cumulative over time, and the toxicity of HMs can pose a threat to humans through a variety of pathways, and yet the development of contamination has been ongoing [6, 7]. Therefore, understanding the extent of heavy metal contamination in soil and identifying its sources are crucial for pollution prevention and control [8].

Sources of HMs in soil systems can be both anthropogenic and natural, and identifying these sources and assessing their ecological risks are important for mitigating the impacts of HMs [9]. The use of self-organiting map (SOM), as a neural network algorithm, can effectively utilize robust imagery and clustering to deal with problems [10], and it has superior performance compared to traditional statistics in handling similarities in complex spatio-temporal variability patterns, SOM can accurately map correlations of HMs [11]. Due to the good performance of SOM in classification and model recognition, the combined use of positive matrix factorization (PMF) may further support the research outcomes of SOM in allocating contributions from different sources. In this study, the integration of SOM and PMF models is likely to be a suitable approach for pollution source identification in Linli County, China. For instance, HOSSAIN et al [12] conducted a survey on sources of heavy metal pollution in Bangladesh using a combination of SOM and PMF methods, identifying four sources of heavy metals and providing an appropriate method for allocating multiple sources of pollution in Bangladesh. DAI et al [13] analyzed the intrinsic elemental relationships of HMs in the study area by means of SOM, and through correlation matrix and principal component analysis, the authors concluded that the probable sources of inputs of Pb, Zn, and Cr were atmospheric or riverine inflow transportation [13]. ZHANG et al [14] categorized the SOM for groundwater source categories and obtained a total of five clusters. BIGDELI et al [15] separately predicted highly favorable regions of geochemical anomaly data for river sediments from the SOM model and concluded that the results of the two models were very similar. Analyzing sources of pollution is a critical step in environmental protection.

After a long period of development and change, the ecological risk assessment system has become the basis for the prevention, understanding and control of pollution in environmental science [16]. The ecological risk assessment methods mainly include qualitative assessment and quantitative assessment. Qualitative assessment has the advantage of being easily understood and implemented, while quantitative assessment is reliable in its evaluation results and has transparent processes. Both methods have been widely used by scholars [17 − 19]. The purpose of this study is to obtain the potential ecological risk status of Linli County. Therefore, to comprehensively consider the impact of different factors on ecological risk, the potential ecological risk index method of quantitative analysis was selected for application. This method helps to comprehensively analyze and compare the risk levels of different elements in Linli County and better understand the overall impact of risks. RUI et al [20] conducted an ecological risk assessment of contaminated elements in an area of Shanghai, China, and found that the contamination had serious negative impacts on the local aquatic environmental system. LIU et al [21] used an ecological assessment system to evaluate soil pollution caused by industrial activities in the Yellow River floodplain, and the results showed that industrial activities had a large impact on bioavailability. The ecological risk assessment system has just become an important pollution evaluation system.

Linli County is located in Changde City, Hunan Province, China, within the transition between the Dongting Lake Basin and the Xuefeng Mountain tectonic zone, and is a comprehensive agricultural county in Hunan Province. Research on this area is limited at present, investigating local environmental safety and ecological risk is critical. Therefore, this study aims to study the environmental pollution in Linli County to provide effective suggestions and evaluation criteria for the future management of the polluted environment in the area. The objectives of this study were to investigate (1) the assessment of contamination status and prediction of spatial distribution of As, Cd, Cr, Cu, Zn, and Pb in the soils of Linli County; (2) the judgment and resolution of sources of HMs

in the soils of Linli County by using SOM and PMF; and (3) the risk of environmental and ecological contamination caused by HMs in the soils of Linli County.

## 2 Materials and methods

### 2.1 Collection and analysis of soil samples

Seventy-four soil samples were collected throughout Linli County in April and June, 2023, respectively. The sampling depth was about 0.2 m, and GPS was used to ensure accurate geographic coordinates. Soil samples preserved in polythene bags were air-dried in the laboratory.

Large soil clods were ground and filtered through a 100-mesh (150 μm) nylon sieve. The filtered soil was thoroughly mixed through a container and then packed in polythene bags and set at 4 ℃. Transfer 0.1 g soil sample into a 50 mL beaker followed by the addition of 6 mL of concentrated nitric acid (6 mol/L) solution and 5 mL of deionized water. Let the beaker sit at room temperature for 4 h, then place it in a water bath and heat it to approximately 60 ℃. Next, place it on a hot plate and heat it at 120−150 ℃ for a digestion time of 1−1.5 h, with a minimum time of 30 min to avoid incomplete decomposition of soil particles and evaporation of nitric acid, until the test solution appears grayish in color and $HNO_3$ has completely evaporated. Remove the test material and add 1 mL of nitric acid and 5 mL of deionized water in a beaker, dissolve the test material and transfer it to a 100 mL volumetric flask and stir in 100 mL of deionized water [22]. The inductively coupled plasma mass spectrometer (ICAP Q) was utilized to examine the concentrations of As, Cr, Cu, Zn and Pb. The main parameters of this instrument include a resolution of 80000 and a sensitivity of 5 with a repetition standard deviation (RSD) of less than 1% [16]. The pH value of soil solution was determined using the electrode method by adding 10 g of sample and 25 mL of carbon dioxide-free distilled water in a beaker with stirring, and the pH value of the solution was determined for 30 min [23]. A 10% blank experiment was set up for each test assay to control to ensure quality control standards. In addition, copper unit powder is used to calibrate instruments and test samples, and calibration curves are prepared to ensure the reliability and accuracy of experimental data.

### 2.2 Pollution evaluation methods

2.2.1 Enrichment factor ($F_E$)

Enrichment factors are used to assess the degree of influence of artificial and natural factors on the contamination of HMs in soil [24]. $F_E$ is defined as follows:

$$F_E=(C_i/C_R)_{sample}/(C_i/C_R)_{background} \quad (1)$$

where $(C_i/C_R)_{sample}$ represents the ratio of the concentration of the study element to that of the reference element, and $(C_i/C_R)_{background}$ is the ratio of the concentration of the study element to the background concentration of the reference element. The background values of As, Cd, Cr, Cu, Zn and Pb were 15.7, 0.126, 71.4, 27.3, 94.4 and 29.7 respectively [23]. Al was chosen as a reference element in this study because of its relatively uniform concentration distribution in the environment. Classification criteria of anthropogenic pollution according to $F_E$: light pollution ($F_E$<2), medium pollution (2<$F_E$<5), high pollution (5<$F_E$<20) and heavy pollution ($F_E$>20) [25]. When the value of $F_E$ tends to 1, then the metal is likely to be of natural origin or from weathering of the earth's crust [26].

2.2.2 Geological cumulative index ($I_{geo}$)

$I_{geo}$ is often used to assess the level of accumulation of HMs in the soil, with the calculation formula chosen:

$$I_{geo}=\log_2 C_r/(1.5B_r) \quad (2)$$

where $C_r$ represents the concentration of element $r$ in the soil and $B_r$ is the background value of element $r$ for the study. The constant 1.5 is used to offset the fluctuating condition of elemental background values in the context of natural conditions. $I_{geo}$ is categorized into 7 classes, i.e., $I_{geo}$≤0, 0−1, 1−2, 2−3, 3 − 4, 4 − 5, ≥5, indicating no pollution, slight pollution, moderate pollution, moderate to heavy pollution, heavy pollution, heavy pollution to severe pollution and severe pollution, respectively [27].

### 2.3 Source analysis methods

2.3.1 Positive matrix factorization

PMF is a receptor model based on matrix decomposition arithmetic, which is often used to assign trace elements to sources because of its skill in performing well in source contribution assignment [28]. The formula is as follows:

$$x_{ij}=\sum_{k=1}^{p}g_{ik}f_{ik}+e_{ij} \tag{3}$$

$$Q=\sum_{i=1}^{m}\sum_{j=1}^{n}\left(e_{ij}/\sigma_{ij}\right)^{2} \tag{4}$$

$$\sigma_{ij}=\frac{5}{6}L_{\mathrm{MD}},\ \left[d\le L_{\mathrm{MD}}\right] \tag{5}$$

$$\sigma_{ij}=\sqrt{\left(\partial_j\times x_{ij}\right)^2+\left(0.5\times L_{\mathrm{MD}}\right)^2},\ \left[d>L_{\mathrm{MD}}\right] \tag{6}$$

The procedure is to obtain the value of $x_{ij}$ by taking the values of $g_{ik}$ and $f_{ik}$, and then adjust the data to obtain the lowest $Q$ value. Where, $x_{ij}$ denotes the concentration of element $j$ in the $i$th sample, $g_{ik}$ denotes the source of element $k$ in the $i$th sample, $f_{ik}$ denotes the concentration of element $j$ in the $k$th sample, $e_{ij}$ is the degree of error, $\sigma_{ij}$ is the uncertainty of element $j$ in the $i$th sample, $\partial_j$ is the relative standard deviation of element $j$, $d$ is the concentration of the study element, and $L_{\mathrm{MD}}$ is the detection limit of the method. $L_{\mathrm{MD}}$ is the detection limit of the detection method.

2.3.2 Self-organizing map networks

The famous SOM algorithm is an unsupervised operation first proposed by Kohonen, also known as the Kohonen map [29]. The SOM network consists of two layers, the input layer and the output layer, with the concentration of each sample element defined as an $n$-dimensional vector of inputs. A vector $\boldsymbol{X}$ is randomly selected, and the Euclidean distance between the neuron and the vector $\boldsymbol{X}$ is computed to accomplish the goal of network training. Then, the neural network is composed by passing through the input layer and is passed to a specific vector of weights. The output layer outputs a plan view of the arrangement sequence of the honeycomb styles (see Figure 1) [30, 31]. The formula for the Euclidean distance ($D_i$) can be expressed as:

$$D_i=\sqrt{\sum_{i=1}^{n}\left[x_i(t)-\omega_{ij}(t)\right]^2}=\|\boldsymbol{X}-\boldsymbol{W}_j\| \tag{7}$$

where $\boldsymbol{W}_j$ is the weight vector of neuron $j$ in the competing layer, $\omega_{ij}$ is the weight between neuron $i$ in the input layer and neuron $j$ in the competing layer, and $n$ is the number of input vectors. During the arithmetic process while considering that there is no suitable rule for the selection of the number of neurons in the input layer, this study will use $m=5\times(n)^{1/2}$ to determine the number of neurons, where $m$ denotes the number of nodes in the self-organizing graph.

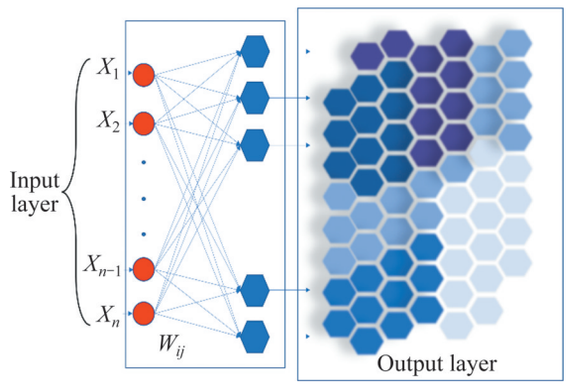


**Figure 1** Schematic of SOM neural network mapping

### 2.4 Ecological risks assessment method

The ecological risk index ($I_{\mathrm{R}}$) is often used to assess the level of ecological risk posed by hazardous factors in the natural environment [32]. The formula is:

$$I_{\mathrm{R}}=\sum E_n^i=\sum T_n^i\times C_n^i \tag{8}$$

where $E_n^i$ is the $I_{\mathrm{R}}$ value of element $i$, $C_n$ is the concentration of the element, and $C_n^i$ is the concentration of the background value of element $i$. $T_n$ is the toxicity response factor (TRF), which corresponds to 10, 30, 2, 5, 1 and 5 for As, Cd, Cr, Cu, Zn and Pb, respectively [33, 34]. Ecological risks are rated as low, medium, high and severe risks, with corresponding index values of $I_{\mathrm{R}}\le150$, 150−300, 300−600 and ≥600, respectively [35].

## 3 Results and discussion

### 3.1 Soil HMs pollution situation

Descriptive analyses of HMs in Linli County soils are shown in Table 1, with HMs data distributed as skewed normal and reported as mean concentrations. The pH values of Linli County soils varied between 4.50 and 8.46, with approximately 59% of the soils having an acidic pH value less than 7 and 41% having an alkaline distribution. As shown in Table 1, the effective mean values of the elements of HMs, except Zn and As, exceeded their corresponding background value concentrations. This result indicates that some of the sampled soils

**Table 1** Descriptive analysis of HMs concentration in soil

| Element | HMs concentration/(mg·kg$^{-1}$) | | | | $C_V$/% | $F_E$ |
|---|---|---|---|---|---|---|
| | Min value | Max value | Mean value | SD | | |
| Cr | 38.9 | 167.6 | 72.5 | 26.3 | 36 | 1.02 |
| Cd | 0.2 | 2.3 | 0.6 | 0.4 | 72 | 4.42 |
| Cu | 17.2 | 77.2 | 30.7 | 9.6 | 31 | 1.12 |
| Zn | 48 | 228.7 | 89.3 | 31 | 35 | 0.95 |
| Pb | 22.3 | 110.4 | 33.6 | 11.1 | 33 | 1.13 |
| As | 6.5 | 32.4 | 12 | 5.45 | 46 | 0.76 |

SD: Standard deviation; $C_V$: the coefficient of variation.

in Linli County were contaminated by Cr, Cd, Cu and Pb to different degrees. In addition, among all samples, the exceedance rates of Zn, As, Cr, Cd, Cu, and Pb were 31.1%, 17.6%, 40.5%, 100%, 56.8% and 63.3%, respectively. Compared to other pollutants, Cd pollution is particularly prominent, with concentrations exceeding background levels in all data samples. The maximum concentration is 182.5 times the background value, and the average concentration is 4.76 times the background value.

The coefficient of variation ($C_V$) is often used to indicate the concentration variability of HMs. $C_V \leq 20\%$, $21\% < C_V \leq 50\%$, $51\% < C_V \leq 100\%$ and $C_V > 100\%$, respectively represent the four grades of low, medium, high and very high variability [36]. From $C_V$, the highest $C_V$ of Cd among all the elements is 76%, which is defined as high variability, while the variability of the rest of the elements falls within the range of medium variability. Higher $C_V$ values indicates that the elements have been affected by the outside world more seriously, so that the high pollutant nature of Cd is mainly caused by the external factors [37, 38]. As shown in Table 1, the average enrichment factor index of Linli County suggests that the $F_E$ values of the remaining elements, except Cd, fall into the light anthropogenic pollution level ($F_E$<2), while the $F_E$ value of Cd is 4.42, reaching medium anthropogenic pollution level. This indicates that the pollution accumulation of Cd is influenced by anthropogenic activities to a greater extent, and this result is consistent with that of $C_V$, which indicates that the source of Cd pollution is mainly caused by anthropogenic activities.

The order of magnitude of the mean $I_{geo}$ of the studied elements in Linn County is as follow: Cd(2.52) >Pb(0.76) >Cu(0.75) >Cr(0.67) >Zn(0.63) > As(0.51). Cd was classified as moderately to heavily polluted, while the rest of the elements were at the level of slightly polluted, indicating that although the overall pollution level of HMs in the soil of Linli County was not high except for Cd, they were affected by pollution, and there were no non-polluting elements in the studied elements. Figure 2 shows the distribution of the ground cumulative index levels for each element. As depicted in Figure 2, Cd and Pb have a small number of non-normal values classified above the moderate to severe pollution levels, indicating that some sampling sites in Linli County are polluted by point sources of HMs [39, 40].

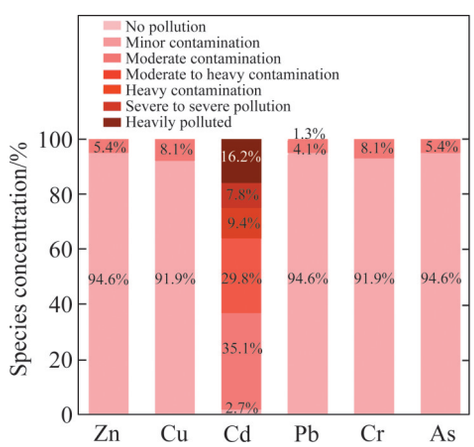


**Figure 2** Distribution of the proportions of each class of the research element $I_{geo}$

### 3.2 Spatial distribution of HMs

Identifying the spatial distribution of HMs in soils in Linli County and discussing areas of HMs enrichment are beneficial for identifying sources of HMs [41]. The distribution of HMs in soil throughout Linli County is shown in Figure 3.

From Figure 3, it can be observed that the distribution of the six HMs exhibits similar features. The concentration of all elements in the southeast direction of the study area is higher, particularly in Linli County, which is rich in industrial activities, leading to higher heavy metal content. Cd is the most polluted element, which shows high concentrations mainly in the northern and southeastern part of the study area. Based on the fieldwork and spatial characteristics, the following conclusions can be drawn: Firstly, the river in the northern part of Linli County provides water for irrigation, and pollution in the upstream water may lead to soil contamination in the surrounding areas

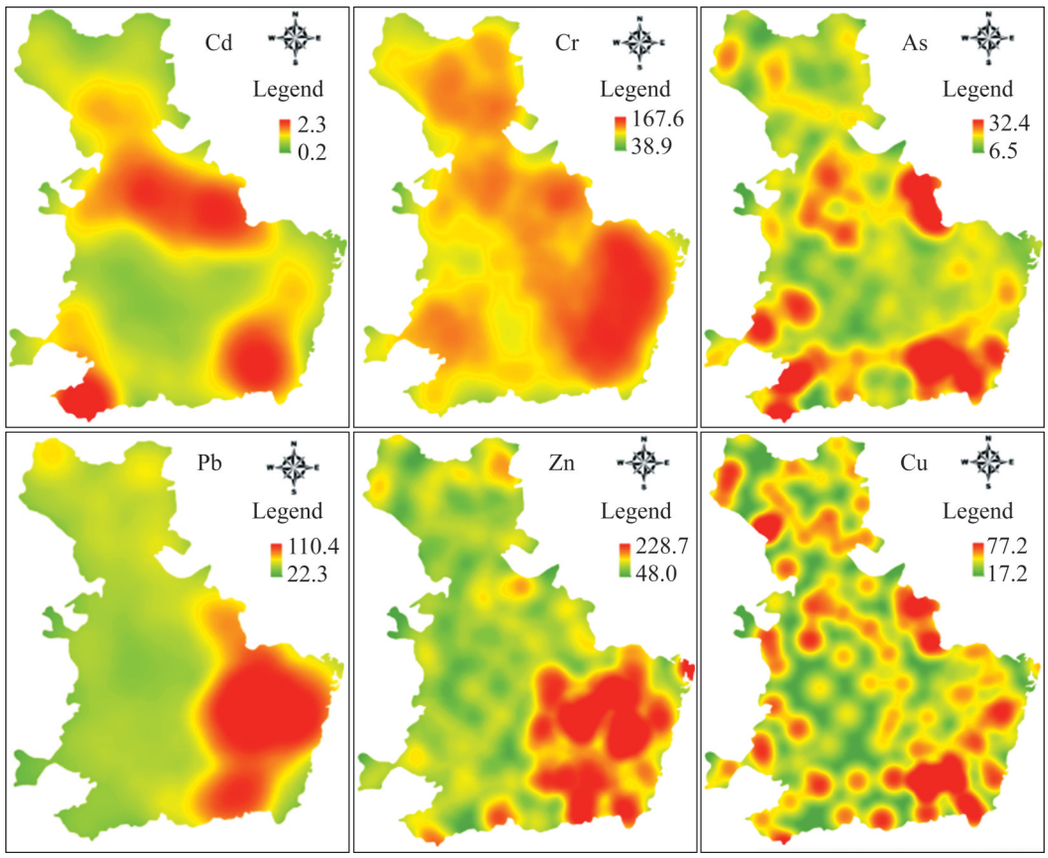


**Figure 3** Schematic diagram of spatial distribution of heavy metals in the study area

[42, 43]; Secondly, as agriculture is the primary industry in Linli County, the use of river water for irrigation and the accompanying use of pesticides and herbicides may lead to Cd enrichment, which then enters the soil through the irrigation water flow, causing pollution [44]; Thirdly, it is possible that accumulated plants serve as a major source of Cd contamination, with the discharge of municipal sewage and industrial wastewater promoting Cd accumulation [45].

The spatial distribution of As closed resembles that of Cd, with high concentrations clustered in the north-central part of Linli County, as well as the southeast and southwest. Similar distribution patterns between elements often indicate a common source of pollution [19]. Additionally, high concentrations of Pb, Zn and Cu are particularly noticeable in the southeast of the study area, primarily concentrated in areas with industrial plant clusters, suggesting industrial activities as a potential cause of HMs accumulation. The high concentration thermograms of Cr cover the entire study area, indicating a relatively wide and irregular spatial distribution, and not limited to a specific area, which suggests a potential natural source for Cr.

### 3.3 Analysis of HMs sources in soil

To investigate the taxonomic relationship between HMs in soil in Linli County and determine the correlation between the studied elements, this study used self-organized maps combined with PMF analysis to conduct competitive output on the concentration and source of HMs at the sampling sites (e.g., Figures 4 and 5).

Based on Figure 4, six elements are displayed in a honeycomb plane format using the self-organizing map (SOM) classification technique. The plane is designed and constructed based on a hue-based classification mode, and the aggregation and allocation of different colors indicate different levels of segmentation for the variable plane. Different network nodes represent different reference values for the input vectors, which are constrained between 0 and 1. Blue indicates low concentration, and pink represents high concentration. When there are

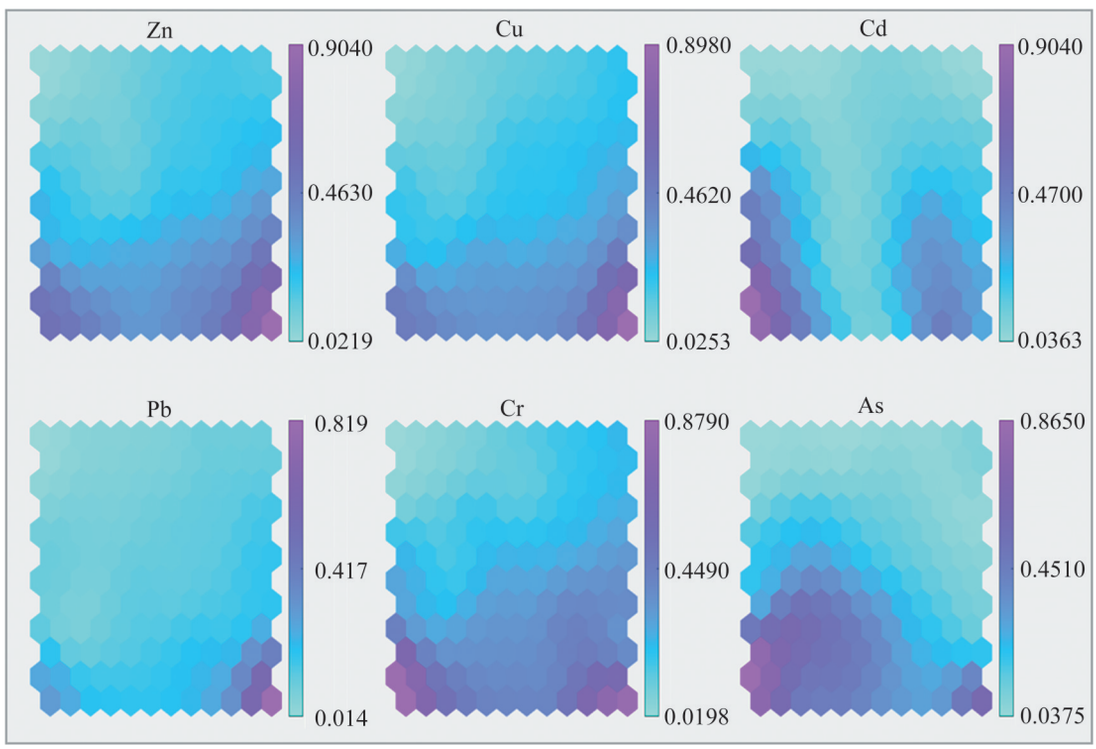


**Figure 4** SOM competitive output cellular network diagram for 6 elements

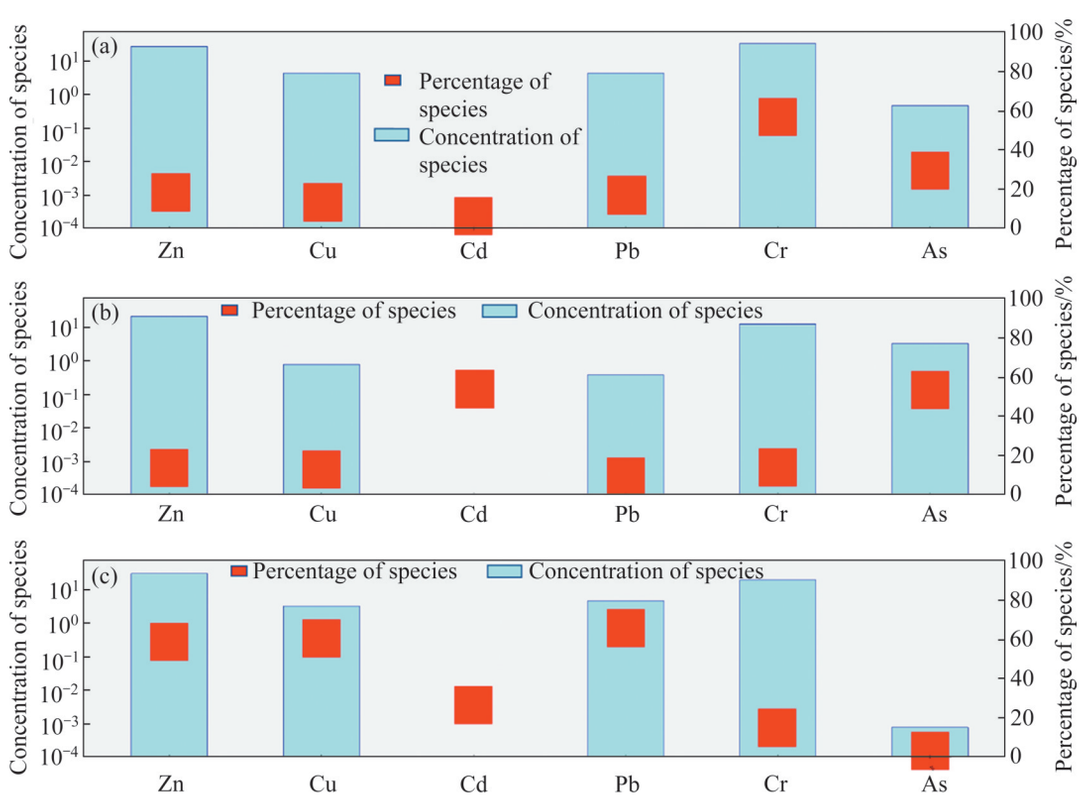


**Figure 5** Distribution map of contribution proportions of each element in factors 1 (a), 2 (b) and 3 (c) in PMF analysis

common or similar relationships among the six elements in the output plane, it indicates that the distribution of the variables is highly correlated [16]. From Figure 4, it can be observed that the classification patterns of Zn, Cu and Pb are highly similar, with all three elements clustered in high concentrations in the lower right corner of the plane. The distribution patterns of Cd and As are more

similar, with a strong correlation observed in the lower left corner of the plane. Cr, on the other hand, is only clustered in the lower left corner. According to the results of SOM analysis, Zn, Cu and Pb distributions exhibit strong correlation, while Cd and As exhibit moderate correlation. Cr is classified as a separate distribution category.

Positive matrix decomposition analysis was carried out for the studied elements within Linli County, and in order to ensure the accuracy of the decomposition, the parameters were adjusted repeatedly, and the concentration and uncertainty were iterated for 20 times, and the optimal solution was derived when the output factor was set to 3 (Figure 5). The fitting coefficients ($R^2$) between the predicted values of the PMF model and the observed values were calculated simultaneously to ensure the applicability of the model. The fitting coefficients for Zn, Cu, Cd, Pb, Cr and As were 0.9917, 0.9528, 0.9276, 0.9626, 0.9670 and 0.9703, respectively. The closer the value of $R^2$ is to 1, the better the fit of the model, indicating that the PMF model is effective in identifying the sources of heavy metal pollution in Linli County.

In factor 1, Cr was used as the representative element with contribution rate of 68.3%. The average concentration of Cr was slightly higher than the background value, but the ground cumulative index indicated that Cr was non-polluted. The spatial distribution of Cr within Linli County was relatively uniform, so the source of Cr was mainly natural weathering, and the concentration of Cr in some of the sampling points might have been affected by industrial and agricultural production, resulting in a concentration higher than the background value [46].

Factor 2 was dominated by Cd (63.6%) and As (62.8%). Both Cd and As exhibited similar spatial distribution patterns and concentration competition models, indicating potential common sources. The enrichment factor suggested that Cd pollution was predominantly caused by anthropogenic sources. Fertilizers and pesticides used in agricultural activities contain high levels of Cd, which contributes to its accumulation. Municipal wastewater from industrial production also contributes to Cd enrichment in soil [43]. At the same time, municipal wastewater from industrial production is also enriched in Cd, and the discharge of this wastewater can lead to the accumulation of Cd in the soil. As in the study, although only a small number of points in the concentration is higher than the background value, but the spatial distribution of As is very similar to that of Cd. Previous studies have shown that the improper use of As herbicides, fertilizers, and pesticides can lead to As accumulation, and the atmospheric deposition of industrial waste gases can accelerate this process, and these factors play important roles in soil development. Despite efforts to reduce exhaust emissions, it is difficult to eliminate this pollution effect [47, 48]. Therefore, the main sources of Cd and As pollution are related to human production activities.

In factor 3, the contributions of Pb, Cu and Zn were 73.5%, 70.6% and 68.7%, respectively. The spatial distribution patterns of the three elements were very similar, and the aggregation areas were all concentrated in the southeast of Linli County. Previous studies have indicated that Pb, Cu and Zn from industrial wastewater can permeate surrounding soil through rivers or pipelines, resulting in soil pollution around water system [22]. Additionally, brake wear, tire wear, and leaded gasoline emissions from automobiles can lead to aggregation of Pb, Cu, and Zn in the soil, and vehicular pollution caused by the transportation of goods in industrial areas may also be responsible for the enrichment of the three elements of Pb, Cu, and Zn in the lower right-hand corner of Linli County [49]. So, factor 3 is a source of pollution due to industrial activities.

The results of SOM and PMF analyses showed a high level of agreement. Overall, the main sources of HMs pollution in Linli County include pollution from production activities, particularly agricultural activities, pollution from natural weathering, and pollution from industrial activities. Among these, human production activities are the primary factor influencing environmental pollution in the surroundings of Linli County.

### 3.4 Ecological risk assessment of soil

The study evaluated the potential ecological risk values of six HMs elements and 74 sampling sites in Linli County, as shown in Figures 6 and 7. The overall ecological pollution in Linli County was predicted using the soil of the sampling sites as the

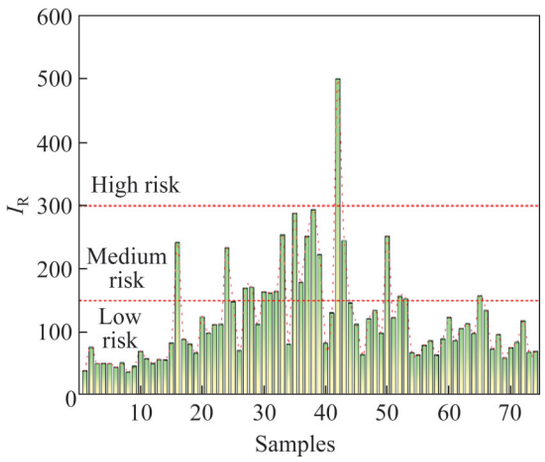


**Figure 6** Schematic diagram of the distribution range and risk level classification of ecological risk values for six elements

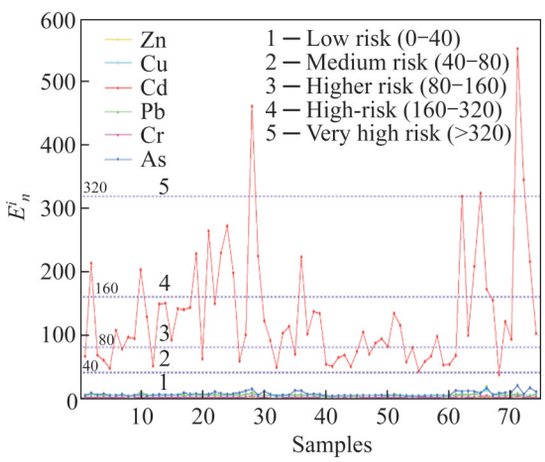


**Figure 7** Distribution range and level division diagram of RI values for 74 sampling points

environmental characteristic value. The maximum and average values of all HMs elements shown in Figure 6, except for Cd, were below 40, indicating that these elements are of low ecological risk in all areas of Linli County (hierarchical classification shown in Figure 6). However, the mean value of ecological risk of Cd was 132.7 (higher risk level), with a maximum of 551.4 (very high-risk level), and the percentage of Cd classified from low to high was 1%, 32%, 38%, 18% and 11%, respectively.

Figure 7 displays the distribution of $I_R$ values of sampling points in Linli County, with values ranging from 59 to 592.8. The ecological risk level in 63.5% of the area is low, while 29.7% of the area reaches a medium-risk pollution level, and the remaining 6.8% of the land exhibits high ecological. This implies that Linli County has an overall low ecological risk level. Cd contributes more than 70% to the medium to high ecological risk class, with minimum and maximum of 71.6% and 94.3%, respectively. This indicates that Cd is the primary element responsible for high ecological risk, mainly due to its low environmental background value and high toxicity response factor. This result is consistent with previous studies that Cd poses the highest ecological risk among HMs in the environment [23, 44].

## 4 Conclusions

This study analyzed the distribution and sources of heavy metal elements in the soil of Linli County, and evaluated their impact on the ecological environment. It revealed the main sources and contamination levels of heavy metal elements in the soil of this area, and confirmed the major contribution of human activities to soil pollution. Based on the research findings, the following priorities were proposed:

1) Cd was the most heavily polluted element. The Cd concentrations in all samples exceeded the environmental background values, with a 100% over-standard rate, and the enrichment factor showed that Cd was moderately artificially polluted. The geo-accumulation index also indicated a moderate to severe contamination level of Cd.

2) The spatial distribution of heavy metals in the soil of Linli County was shown, and the areas where heavy metals were enriched were identified. The results indicated that the distribution patterns of all elements were generally the same in the study area, and that Cd was the most heavily polluted element, mainly distributed in the northern and southeastern parts of the study area. In addition, regarding the possible sources of contaminants, this study analyzed the factors of water pollution, agricultural activities and industrial activities.

3) SOM analysis showed that the distribution of Zn, Cu and Pb had a strong correlation, while Cd and As had a moderate correlation, and Cr was a separate distribution category. The PMF analyzed three pollution sources, namely, production activity pollution sources primarily from agricultural activities, pollution sources primarily from natural weathering, and pollution sources caused industrial activities.

4) In Linli County, 63.5% of the region was classified as low ecological risk level, 29.7% were classified as moderate risk level of pollution, and 6.8% of the land was classified as high ecological risk level of pollution. The contribution rate of Cd to the middle and high ecological risk levels was over 70%, with a minimum of 71.6% and a maximum of 94.3%.

This study has important implications for the producers to reduce heavy metal pollution in the soil of Linli County and its harm to the ecosystem. The findings also provide important references and methods for similar research in the future.

## Contributors

ZOU Hao: Methodology, Formal analysis, Data curation, Writing-original draft & Editing and Visualization, Investigation. LI Wu-qing: Methodology, Writing-Original, Investigation, Data curation. REN Bo-zhi: Conceptualization, Supervision. XIE Qing: Methodology. CHEN Lu-yuan: Data curation; CAI Zhao-qi: Investigation, Resources. WANG Jin: Language censorship.

## Conflict of interest

ZOU Hao, LI Wu-qing, REN Bo-zhi, XIE Qing, CHEN Lu-yuan, CAI Zhao-qi and WANG Jin declare that they have no conflict of interest.

## References

[1] DODD M, AMPONSAH L O, GRUNDY S, et al. Human health risk associated with metal exposure at Agbogbloshie e-waste site and the surrounding neighbourhood in Accra, Ghana [J]. Environmental Geochemistry and Health, 2023, 45(7): 4515−4531. DOI: 10.1007/s10653-023-01503-0.

[2] ZHANG Chao, WANG Xing, JIANG Shi-hao, et al. Heavy metal pollution caused by cyanide gold leaching: A case study of gold tailings in central China [J]. Environmental Science and Pollution Research International, 2021, 28(23): 29231−29240. DOI: 10.1007/s11356-021-12728-w.

[3] GAO Jing, WANG Lu-cang. Ecological and human health risk assessments in the context of soil heavy metal pollution in a typical industrial area of Shanghai, China [J]. Environmental Science and Pollution Research International, 2018, 25(27): 27090 − 27105. DOI: 10.1007/s11356-018-2705-8.

[4] LONG Zhi-jie, HUANG Yi, ZHANG Wei, et al. Effect of different industrial activities on soil heavy metal pollution, ecological risk, and health risk [J]. Environmental Monitoring and Assessment, 2021, 193(1): 20. DOI: 10.1007/s10661-020-08807-z.

[5] XIANG Ming-tao, LI Yan, YANG Jia-yu, et al. Assessment of heavy metal pollution in soil and classification of pollution risk management and control zones in the industrial developed city [J]. Environmental Management, 2020, 66(6): 1105−1119. DOI: 10.1007/s00267-020-01370-w.

[6] SOLGI E, ESMAILI-SARI A, RIYAHI-BAKHTIARI A, et al. Soil contamination of metals in the three industrial estates, Arak, Iran [J]. Bulletin of Environmental Contamination and Toxicology, 2012, 88(4): 634 − 638. DOI: 10.1007/s00128-012-0553-7.

[7] SPRAGUE D D, VERMAIRE J C. Legacy arsenic pollution of lakes near cobalt, Ontario, Canada: Arsenic in lake water and sediment remains elevated nearly a century after mining activity has ceased [J]. Water, Air, & Soil Pollution, 2018, 229(3): 87. DOI: 10.1007/s11270-018-3741-1.

[8] OUYANG Wei, WANG Yi-di, LIN Chun-ye, et al. Heavy metal loss from agricultural watershed to aquatic system: A scientometrics review [J]. The Science of the Total Environment, 2018, 637 − 638: 208 − 220. DOI: 10.1016/j.scitotenv.2018.04.434.

[9] WU Hui-hui, XU Cong-bin, WANG Jin-hang, et al. Health risk assessment based on source identification of heavy metals: A case study of Beiyun River, China [J]. Ecotoxicology and Environmental Safety, 2021, 213: 112046. DOI: 10.1016/j.ecoenv.2021.112046.

[10] WANG Zhan, XIAO Jun, WANG Ling-qing, et al. Elucidating the differentiation of soil heavy metals under different land uses with geographically weighted regression and self-organizing map [J]. Environmental Pollution, 2020, 260: 114065. DOI: 10.1016/j.envpol.2020.114065.

[11] NAKAGAWA K, YU Zhi-qiang, BERNDTSSON R, et al. Temporal characteristics of groundwater chemistry affected by the 2016 Kumamoto earthquake using self-organizing maps [J]. Journal of Hydrology, 2020, 582: 124519. DOI: 10.1016/j.jhydrol.2019.124519.

[12] HOSSAIN BHUIYAN M A, CHANDRA KARMAKER S, BODRUD-DOZA M, et al. Enrichment, sources and ecological risk mapping of heavy metals in agricultural soils of Dhaka district employing SOM, PMF and GIS methods [J]. Chemosphere, 2021, 263: 128339. DOI: 10.1016/j.chemosphere.2020.128339.

[13] DAI Li-jun, WANG Ling-qing, LI Lian-fang, et al. Multivariate geostatistical analysis and source identification of heavy metals in the sediment of Poyang Lake in China [J]. The Science of the Total Environment, 2018, 621: 1433 − 1444. DOI: 10.1016/j.scitotenv.2017.10.085.

[14] ZHANG Yao-bin, ZHANG Qiu-lan, CHEN Wen-fang, et al. Hydrogeochemical analysis and groundwater pollution source identification based on self-organizing map at a contaminated site [J]. Journal of Hydrology, 2023, 616: 128839. DOI: 10.1016/j.jhydrol.2022.128839.

[15] BIGDELI A, MAGHSOUDI A, GHEZELBASH R. Application of self-organizing map (SOM) and K-means clustering algorithms for portraying geochemical anomaly patterns in Moalleman district, NE Iran [J]. Journal of Geochemical Exploration, 2022, 233: 106923. DOI: 10.1016/j.gexplo.2021.106923.

[16] ZOU Hao, REN Bo-zhi. Analyzing topsoil heavy metal pollution sources and ecological risks around antimony mine

waste sites by a joint methodology [J]. Ecological Indicators, 2023, 154: 110761. DOI: 10.1016/j.ecolind.2023.110761

[17] WANG Ya-zhu, DUAN Xue-jun, WANG Lei. Spatial distribution and source analysis of heavy metals in soils influenced by industrial enterprise distribution: Case study in Jiangsu Province [J]. The Science of the Total Environment, 2020, 710: 134953. DOI: 10.1016/j.scitotenv.2019.134953.

[18] XIANG Long, LIU Ping-hui, JIANG Xing-fu, et al. Health risk assessment and spatial distribution characteristics of heavy metal pollution in rice samples from a surrounding hydrometallurgy plant area in No. 721 uranium mining, East China [J]. Journal of Geochemical Exploration, 2019, 207: 106360. DOI: 10.1016/j.gexplo.2019.106360.

[19] XUE Sheng-guo, WANG Yuan-yuan, JIANG Jun, et al. Groundwater heavy metal(loid)s risk prediction based on topsoil contamination and aquifer vulnerability at a zinc smelting site [J]. Environmental Pollution, 2024, 341: 122939. DOI: 10.1016/j.envpol.2023.122939.

[20] RUI Xuan, GONG Hua-bo, YUAN Hai-ping, et al. Distribution, removal and ecological risk assessment of antibiotics in leachate from municipal solid waste incineration plants in Shanghai, China [J]. The Science of the Total Environment, 2023, 900: 165894. DOI: 10.1016/j.scitotenv.2023.165894.

[21] LIU Fu-tian, WANG Xue-qiu, DAI Shuang, et al. Impact of different industrial activities on heavy metals in floodplain soil and ecological risk assessment based on bioavailability: A case study from the Middle Yellow River Basin, northern China [J]. Environmental Research, 2023, 235: 116695. DOI: 10.1016/j.envres.2023.116695

[22] JIANG Feng, REN Bo-zhi, HURSTHOUSE A, et al. Distribution, source identification, and ecological-health risks of potentially toxic elements (PTEs) in soil of thallium mine area (southwestern Guizhou, China) [J]. Environmental Science and Pollution Research International, 2019, 26(16): 16556−16567. DOI: 10.1007/s11356-019-04997-3.

[23] ZOU Hao, REN Bo-zhi, DENG Xin-ping, et al. Geographic distribution, source analysis, and ecological risk assessment of PTEs in the topsoil of different land uses around the antimony tailings tank: A case study of Longwangchi tailings pond, Hunan, China [J]. Ecological Indicators, 2023, 150: 110205. DOI: 10.1016/j.ecolind.2023.110205.

[24] NAZZAL Y, ZAIDI F K, ABUAMARAH B A, et al. Evaluation of metals that are potentially toxic to agricultural surface soils, using statistical analysis, in northwestern Saudi Arabia [J]. Environmental Earth Sciences, 2016, 75(2): 171. DOI: 10.1007/s12665-015-4800-1.

[25] LI Chu-xuan, LI Mu, ZENG Jia-qing, et al. Migration and distribution characteristics of soil heavy metal(loid)s at a lead smelting site [J]. Journal of Environmental Sciences, 2024, 135: 600−609. DOI: 10.1016/j.jes.2023.02.007.

[26] RASHED M N. Monitoring of contaminated toxic and heavy metals, from mine tailings through age accumulation, in soil and some wild plants at Southeast Egypt [J]. Journal of Hazardous Materials, 2010, 178(1 − 3): 739 − 746. DOI: 10.1016/j.jhazmat.2010.01.147.

[27] XIE Qing, REN Bo-zhi, SHI Xi-yang, et al. Factors on the distribution, migration, and leaching of potential toxic metals in the soil and risk assessment around the zinc smelter [J]. Ecological Indicators, 2022, 144: 109502. DOI: 10.1016/j.ecolind.2022.109502.

[28] MAO Ling-chen, LIU Li-bo, YAN Nan-xia, et al. Factors controlling the accumulation and ecological risk of trace metal(loid)s in river sediments in agricultural field [J]. Chemosphere, 2020, 243: 125359. DOI: 10.1016/j.chemosphere.2019.125359.

[29] KEBONYE N M, EZE P N, JOHN K, et al. Self-organizing map artificial neural networks and sequential Gaussian simulation technique for mapping potentially toxic element hotspots in polluted mining soils [J]. Journal of Geochemical Exploration, 2021, 222: 106680. DOI: 10.1016/j. gexplo.2020.106680.

[30] WU Jia-jun, HUANG Zheng, QIAO Hong-chao, et al. Prediction about residual stress and microhardness of material subjected to multiple overlap laser shock processing using artificial neural network [J]. Journal of Central South University, 2022, 29(10): 3346−3360. DOI: 10.1007/s11771-022-5158-7.

[31] LI Tao, SUN Gui-hua, YANG Chu-peng, et al. Using self-organizing map for coastal water quality classification: Towards a better understanding of patterns and processes [J]. The Science of the Total Environment, 2018, 628−629: 1446−1459. DOI: 10.1016/j.scitotenv.2018.02.163.

[32] FEI Jiang-chi, MIN Xiao-bo, WANG Zhen-xing, et al. Health and ecological risk assessment of heavy metals pollution in an antimony mining region: A case study from South China [J]. Environmental Science and Pollution Research International, 2017, 24(35): 27573 − 27586. DOI: 10.1007/s11356-017-0310-x.

[33] CHEN Zhen-yu, ROAD D, ZHAO Yuan-yi, et al. Ecological risk assessment and cumulative early warning of heavy metals in the soils near the Luanchuan molybdenum polymetallic ore concentration area, Henan [J]. China Geology, 2023.. DOI: 10.31035/cg2023003

[34] VICTOR T L, DAVID M. Ecological risk of trace metals in soil from gold mining region in South Africa [J]. Journal of Hazardous Materials Advances, 2022, 7: 100118. DOI: 10.1016/J.HAZADV.2022.100118.

[35] CAO Jie, XIE Cheng-yu, HOU Zhi-ru. Ecological evaluation of heavy metal pollution in the soil of Pb-Zn mines [J]. Ecotoxicology, 2022, 31(2): 259−270. DOI: 10.1007/s10646-021-02505-3.

[36] LV Jian-shu, LIU Yang, ZHANG Zu-lu, et al. Factorial Kriging and stepwise regression approach to identify environmental factors influencing spatial multi-scale variability of heavy metals in soils [J]. Journal of Hazardous Materials, 2013, 261: 387 − 397. DOI: 10.1016/j. jhazmat.2013.07.065.

[37] DENG Yan, JIANG Lu-hua, XU Liang-feng, et al. Spatial distribution and risk assessment of heavy metals in contaminated paddy fields - A case study in Xiangtan City, Southern China [J]. Ecotoxicology and Environmental Safety, 2019, 171: 281 − 289. DOI: 10.1016/j. ecoenv. 2018.12.060.

[38] FENG Zhao-hui, DENG Li, GUO Yi-kai, et al. The spatial analysis, risk assessment and source identification for mercury in a typical area with multiple pollution sources in Southern China [J]. Environmental Geochemistry and

Health, 2023, 45(6): 4057−4069. DOI: 10.1007/s10653-022-01436-0.

[39] LIU Hai-wei, ZHANG Yan, YANG Jia-shuo, et al. Quantitative source apportionment, risk assessment and distribution of heavy metals in agricultural soils from southern Shandong Peninsula of China [J]. Science of the Total Environment, 2021, 767: 144879. DOI: 10.1016/j.scitotenv.2020.144879.

[40] HAO Xin-rui, YI Xiao-yun, DANG Zhi, et al. Heavy metal sources, contamination and risk assessment in legacy Pb/Zn mining tailings area: Field soil and simulated rainfall [J]. Bulletin of Environmental Contamination and Toxicology, 2022, 109(4): 636−642. DOI: 10.1007/s00128-022-03555-x.

[41] HE Ying-ping, HAN Zhi-wei, WU Fu-zhong, et al. Spatial distribution and environmental risk of arsenic and antimony in soil around an antimony smelter of Qinglong County [J]. Bulletin of Environmental Contamination and Toxicology, 2021, 107(6): 1043 − 1052. DOI: 10.1007/s00128-021-03118-6.

[42] JIANG Feng, REN Bo-zhi, HURSTHOUSE A, et al. Evaluating health risk indicators for PTE exposure in the food chain: Evidence from a thallium mine area [J]. Environmental Science and Pollution Research, 2020, 27(19): 23686−23694. DOI: 10.1007/s11356-020-08733-0.

[43] REHMAN M Z U, RIZWAN M, HUSSAIN A, et al. Alleviation of cadmium (Cd) toxicity and minimizing its uptake in wheat (Triticum aestivum) by using organic carbon sources in Cd-spiked soil [J]. Environmental Pollution, 2018, 241: 557−565. DOI: 10.1016/j.envpol.2018.06.005.

[44] XUE Sheng-guo, KE Wen-shun, ZENG Jia-qing, et al. Pollution prediction for heavy metals in soil-groundwater systems at smelting sites [J]. Chemical Engineering Journal, 2023, 473: 145499. DOI: 10.1016/j.cej.2023.145499.

[45] KE Wen-shun, LI Chu-xuan, ZHU Feng, et al. The assembly process and co-occurrence patterns of soil microbial communities at a lead smelting site [J]. The Science of the Total Environment, 2023, 894: 164932. DOI: 10.1016/j.scitotenv.2023.164932.

[46] LUO Lei, MA Yi-bing, ZHANG Shu-zhen, et al. An inventory of trace element inputs to agricultural soils in China [J]. Journal of Environmental Management, 2009, 90(8): 2524−2530. DOI: 10.1016/j.jenvman.2009.01.011.

[47] XIAO Ran, GUO Di, ALI A, et al. Accumulation, ecological-health risks assessment, and source apportionment of heavy metals in paddy soils: A case study in Hanzhong, Shaanxi, China [J]. Environmental Pollution, 2019, 248: 349 − 357. DOI: 10.1016/j.envpol.2019.02.045.

[48] TIAN He-zhong, ZHOU Jun-rui, ZHU Chuan-yong, et al. A comprehensive global inventory of atmospheric Antimony emissions from anthropogenic activities, 1995-2010 [J]. Environmental Science & Technology, 2014, 48(17): 10235−10241. DOI: 10.1021/es405817u.

[49] CHEN Chao, ZHOU Jian. A new empirical chart for coal burst liability classification using Kriging method [J]. Journal of Central South University, 2023, 30(4): 1205 − 1216. DOI: 10.1007/s11771-023-5294-8.

**(Edited by HE Yun-bin)**

## 中文导读

### 重金属污染与生态风险评价—基于自组织地图和正矩阵分解的临澧县土壤研究

**摘要：**土壤重金属污染一直是环境科学中备受关注的问题。本文对中国临澧县土壤中六种重金属(As、Cd、Cr、Cu、Zn和Pb)的污染水平、分布、来源及其对生态环境的影响进行了分析。样本浓度分析结果显示Cd的浓度均超过背景值，超标率达到100%，其余元素的平均浓度与背景值相近，超标率均在13.5%以下。地累计指数和富集因子指数均显示Cd是污染最严重的元素，其他元素则处于轻度污染级别以下。自组织地图(SOM)和正矩阵分解(PMF)的分析结果显示农业活动是土壤中重金属元素主要来源之一，而自然风化和工业污染也会导致土壤污染。Cd是临澧县土壤中污染最显著的元素，对生态环境造成的影响最大，达到较高风险等级。本研究为降低土壤重金属污染和生态环境风险提供了重要参考，同时也为相关部门制定有效的污染防治、生态环境保护政策提供了理论指导。

**关键词：**生态风险；正矩阵分解；重金属污染；土壤；自组织地图